^{18}F-Sodium Fluoride PET: History, Technical Feasibility, Mechanism of Action, Normal Biodistribution, and Diagnostic Performance in Bone Metastasis Detection Compared with Other Imaging Modalities

Kriti Ahuja[1], Houman Sotoudeh[1], Samuel J. Galgano[1], Ramandeep Singh[2], Nishant Gupta[3], Siddhartha Gaddamanugu[1], and Gagandeep Choudhary[1]

[1]Department of Radiology, University of Alabama at Birmingham, Birmingham, Alabama; [2]Department of Radiology, Massachusetts General Hospital, Boston, Massachusetts; and [3]Department of Radiology, Columbia University at Bassett Healthcare, Cooperstown, New York

CE credit: For CE credit, you can access the test for this article, as well as additional *JNMT* CE tests, online at https://www.snmmilearningcenter.org. Complete the test online no later than March 2023. Your online test will be scored immediately. You may make 3 attempts to pass the test and must answer 80% of the questions correctly to receive 1.0 CEH (Continuing Education Hour) credit. SNMMI members will have their CEH credit added to their VOICE transcript automatically; nonmembers will be able to print out a CE certificate upon successfully completing the test. The online test is free to SNMMI members; nonmembers must pay $15.00 by credit card when logging onto the website to take the test.

The skeleton is the third most common site for metastasis overall, after the lungs and liver. Accurate diagnosis of osseous metastasis is critical for initial staging, treatment planning, restaging, treatment monitoring, and survival prediction. Currently, ^{99m}Tc-methylene diphosphonate whole-body scanning is the cornerstone of imaging to detect osseous metastasis. Although ^{18}F-sodium fluoride (^{18}F-NaF) was one of the oldest medical tracers for this purpose, it was replaced by other tracers because of their better physical properties, until recently. Continued development of PET scanners has opened a new era for ^{18}F-NaF, and given its higher sensitivity, there have been increasing applications in imaging. In this review, we will discuss the history, technical aspects, radiobiology, and biodistribution of this tracer. Finally, we compare the accuracy of ^{18}F-NaF PET with other conventional imaging methods for detection of osseous metastasis.

Key Words: ^{18}F-sodium fluoride; PET/CT; bone scan; bone metastases; ^{99m}Tc-methylene diphosphonate

J Nucl Med Technol 2020; 48:9–16
DOI: 10.2967/jnmt.119.234336

The most common primaries for bony metastasis are breast and prostate cancers followed by pulmonary, renal, and thyroid malignancies. Appropriate diagnosis of bone metastasis is critical for initial staging, restaging, treatment monitoring, and survival prediction. Currently, whole-body scintigraphy and SPECT with ^{99m}Tc-methylene diphosphonate (^{99m}Tc-MDP) is the imaging standard for detection of osseous metastasis. ^{18}F-sodium fluoride (^{18}F-NaF) is a positron-emitting radiopharmaceutical used for skeletal imaging. It provides diagnostic information superior to that of ^{99m}Tc-MDP bone scans due to higher sensitivity and specificity in a wide variety of osseous metastasis (*1*). Combined information provided by PET and CT not only confers superiority in the characterization of malignant and benign processes but also reduces the additional imaging work-up, thus preventing diagnostic delays. Image quality, multiplanar information, and anatomic localization are further improved with the better spatial resolution of modern equipment and scanners. Previous work, including multiple case series, clinical trials, and metaanalyses, have demonstrated the advantages of ^{18}F-NaF PET/CT for the detection, evaluation, and treatment planning of bony metastasis (*2–12*). In this article, we have discussed the history, technical aspects, mechanism of action, radiobiology, and comparative diagnostic performance of ^{18}F-NaF with ^{99m}Tc-MDP bone scanning, ^{18}F-FDG PET, CT, and MRI.

HISTORY

^{18}F-NaF, one of the oldest radiopharmaceuticals, became standard for nuclear bone imaging in the 1960s using conventional γ-cameras, before the availability of PET scanners. In the 1970s it was largely replaced by ^{99m}Tc-labeled compounds because of their better physical characteristics (e.g., longer half-life and lower photon energy) for imaging with γ-cameras (*13*). ^{18}F-NaF was initially approved by the U.S. Food and Drug Administration in 1972 for bone scintigraphy but was subsequently withdrawn in 1975 for nonclinical reasons. In the 1990s, with the advent of whole-body PET scanners, it became

Received Jul. 31, 2019; revision accepted Oct. 30, 2019.
For correspondence or reprints contact: Gagandeep Choudhary, Department of Radiology, University of Alabama at Birmingham, 619 19th St. S., JT779, Birmingham, AL 35249.
E-mail: gchoudhary@uabmc.edu
Published online Dec. 6, 2019.

possible to obtain high-resolution and high-contrast imaging using ^{18}F-NaF. This led to the return of ^{18}F-NaF in 1993 for diagnostic imaging, followed by Food and Drug Administration approval in 2000. Progressive development, the growing availability of PET/CT scanners, and years of shortage of ^{99}Mo–^{99}Tc generators led to further interest in ^{18}F-NaF. In 2011, it was approved by the Centers for Medicare and Medicaid Services under the National Oncologic PET Registry for detection of osseous metastasis (*1*). The registry was closed to accrual on December 14, 2017, with over 65,000 ^{18}F-NaF PET scans performed on Medicare beneficiaries (*14,15*). As of this writing, the Centers for Medicare and Medicaid Services is not reimbursing ^{18}F-NaF PET/CT scans on Medicare beneficiaries. Failure of approval by the Centers for Medicare and Medicaid Services was due to the inability of various clinical studies to address the impact of ^{18}F-NaF PET on palliative or curative care, survival, or quality of care (*15*). This article not only will review the superior image quality demonstrated by ^{18}F-NaF PET but also will serve as a reference for documenting the benefits of ^{18}F-NaF PET over bone scanning.

TECHNICAL ASPECTS

^{18}F is produced by bombarding ^{18}O-enriched water with high-energy protons in a cyclotron. The carrier-free ^{18}F produced is eluted with 0.9% sodium chloride solution, resulting in formation of ^{18}F-NaF. Once produced, the ^{18}F-NaF is commercially available as an isotonic, sterile, colorless, pyrogen-free solution. The ^{18}F has a half-life of 109.7 min and decays into stable ^{18}O with ejection of a positron from the nucleus. This ejected positron annihilates with an electron, producing two 511-keV photons. PET imaging is possible because of these 2 photons, which are emitted at about 180° from one another. Whereas the ^{99m}Tc is generator-produced with a half-life of 6 h, ^{99m}Tc-MDP is manufactured by mixing ^{99m}Tc-sodium pertechnetate with commercially available MDP kits.

Patient preparation is crucial before any imaging study. Unlike ^{18}F-FDG, ^{18}F-NaF does not require patients to be in a fasting state; they can take all their usual medications. Good hydration and frequent urination are strongly recommended to promote tracer excretion, which results in a lower radiation dose and better image quality. With ^{18}F-NaF, images can be obtained as early as 30–45 min after injection. However, as compared with ^{99m}Tc-MDP, the effective radiation dose for ^{18}F-NaF is higher. For example, about a 370-MBq (10 mCi) dose of ^{18}F-NaF delivers 8.9 mSv to an adult patient, which is approximately 70% higher than the typical ^{99m}Tc-MDP dose (*16*). When the accompanying attenuation correction low-dose CT is used, the effective radiation dose is usually less than 10 mSv. By convention, as with other radiopharmaceutical agents, ^{18}F-NaF PET/CT should be avoided in pregnant patients, unless the potential benefits outweigh the radiation risk to the mother and fetus. During lactation, interruption of breastfeeding is not advisable (*16,17*). Thus, there are potential risks and benefits associated with administration of ^{18}F-NaF that must be considered before patients are selected for imaging (Table 1).

MECHANISM OF ACTION AND RADIOBIOLOGY

The ^{18}F-NaF uptake mechanism in the bones is similar to that for ^{99m}Tc-MDP but with better pharmacokinetics, faster clearance from blood, and higher uptake in the bones. ^{18}F-NaF has minimal protein binding, which allows for a high first-pass extraction and fast soft-tissue clearance (*18*). Approximately 50% of the injected tracer is taken up by the bones immediately after injection (*19*). Uptake of ^{18}F-NaF in a bone undergoing remodeling is 10 times that in normal bone (*20*). The remaining tracer is rapidly cleared from plasma and excreted by the kidneys, with only 10% of the tracer remaining in the blood after 1 h, resulting in a very high bone-to-background contrast. The low protein binding and decreased background uptake allow ^{18}F-NaF PET scanning to be done 1 h after administration of the radiotracer, earlier than for ^{99m} Tc-MDP scanning, which is typically 3–4 h after injection. The urinary bladder receives the highest radiation dose, followed by osteogenic cells and red marrow, respectively. ^{18}F-NaF binds to areas of new bone formation and is a marker of blood flow and osteoblastic activity, with blood flow being the rate-limiting step for uptake (*13,17*). The mechanism of uptake for ^{18}F-NaF in the bones is similar to that for ^{99m}Tc-MDP. Bone deposition occurs via chemisorption, in which the OH^- ions in hydroxyapatite are exchanged for $^{18}F^-$ ions, converting hydroxyapatite to fluorapatite. Though the uptake mechanisms of ^{18}F-NaF and ^{99m}Tc-MDP are similar, they exhibit differences in pharmacokinetics and radiobiology characteristics.

TABLE 1
Comparison Table Between ^{18}F-NaF and ^{99m}Tc-MDP (*1,17*)

Characteristic	^{18}F-NaF	^{99m}Tc-MDP
Production	Cyclotron	Generator
Half-life	109.7 min	6 h
Photon energy	511 keV	140 keV
Spatial resolution	Higher (4–5 mm)	Lower
Critical organ	Urinary bladder	Bones
Typical dose	185–370 MBq (5–10 mCi)	740–1,100 MBq (20–30 mCi)
Injection to imaging time	30–60 min	3–4 h
Effective dose	8.9 mSv (370 MBq [10 mCi])	5.3 mSv (925 MBq [25 mCi])

NORMAL BIODISTRIBUTION

The biodistribution of ^{18}F-NaF is dependent on the differential regional blood flow and target organs (Fig. 1). The 2 primary target organs for ^{18}F-NaF uptake are the skeleton and urinary bladder (*21*). Though ^{18}F-NaF demonstrates uniform tracer distribution in bones, the non-homogeneous patterns in adults are attributable to differences in regional blood flow and bone crystal surface area. Comparatively, in children and adolescents, intense and symmetric tracer uptake can be seen in the metaphysis. Urinary washout is the major route of excretion and leads to the visualization of kidneys, ureter, and urinary bladder. The intensity of tracer in the urinary tract depends on renal function, hydration state, and the interval between tracer injection and imaging acquisition. Hyperemia in the soft tissue can cause soft-tissue uptake. Active sclerotic lesions have diffuse increased uptake. An osteolytic lesion or lesion with minimal osteoblastic reaction can show a variable level of uptake, ranging from undetectable to a rim of activity to intense uptake. However, the mechanism of uptake is not limited to neoplastic processes, as any process, benign or malignant, that causes bone remodeling and increased turnover will show increased uptake. In the past, the degree of uptake was not considered sufficient to distinguish between benign and malignant lesions. Therefore, SUVs were not routinely used in the interpretation of ^{18}F-NaF PET/CT scans (*17,18*). Although there seems to be controversy on the differentiation of benign from malignant bone lesions based on SUV, several reports indicate that an SUV_{max} of 55–100 is concerning for a malignant process, whereas degenerative changes typically have an SUV_{max} of less than 50 (*22–24*). Also, the pattern of uptake may be characteristic or suggestive of a specific etiology, and the CT component of PET/CT is helpful in localizing and differentiating malignant from benign conditions.

The dose of ^{18}F-NaF for PET/CT is 148–370 MBq (40–100 μCi)/kg in adults, with the maximum dose being 370 MBq (10 mCi). Given the smaller administered dose and shorter half-life of ^{18}F-NaF, the absorbed dose of ^{18}F-NaF is similar to that of ^{99m}Tc-MDP (*17,18,21,25*). Although images may be obtained as early as 30–45 min after injection of ^{18}F-NaF, it is preferable to wait for about 1–1.5 h for better image quality. The recommended imaging protocol for ^{18}F-NaF PET is beyond the scope of this article, and readers are referred to the protocol guideline of the Society of Nuclear Medicine and Molecular Imaging (*17*).

COMPARISON

^{18}F-NaF Versus ^{99m}Tc-MDP

In comparison to the ^{99m}Tc-MDP whole-body scan, ^{18}F-NaF has better image quality because of better spatial resolution (4–5 mm), higher target-to-background ratio, and higher overall sensitivity in lesion detection (*17,26*). The increased spatial resolution of ^{18}F-NaF PET is especially helpful for detection of small metastases in the spine (Fig. 2).

A major diagnostic application of ^{18}F-NaF PET scan that has been explored is its use in the detection of osseous lesions of metastatic cancers such as breast, prostate, and lung cancers. With growing research on the relevance of ^{18}F-NaF PET in the field of oncology, it has been proven to be an important tool when compared with traditional modalities such as planar and SPECT ^{99m}Tc-MDP bone scintigraphy in assessing the extent of metastatic burden for a variety of malignancies (*9–11,27–40*).

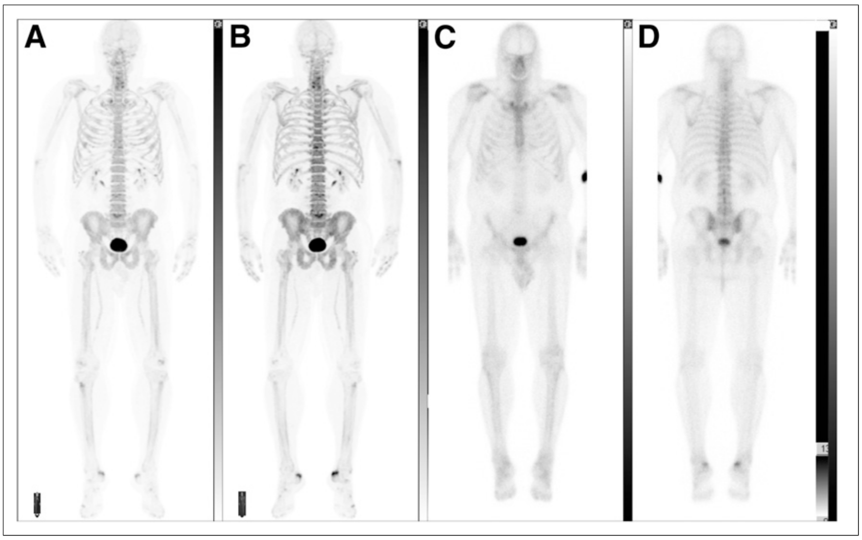

FIGURE 1. A 66-y-old man with history of prostate adenocarcinoma, seen for evaluation of bony metastasis after androgen deprivation therapy and definitive radiotherapy. (A and B) Anterior and posterior maximum-intensity projections of ^{18}F-NaF PET scan show normal physiologic biodistribution. Mild scattered degenerative changes are seen in spine. (C and D) Anterior and posterior views of whole-body ^{99m}Tc-MDP bone scan of same patient performed 3 wk earlier show normal physiologic biodistribution. Both scans show no metastatic lesions.

There is evidence that ^{18}F-NaF PET can be positive earlier than ^{99m}Tc-MDP whole-body bone scanning in small lytic or blastic metastases (*33*). A meta-analysis of various studies also compared these modalities and found ^{18}F-NaF PET/CT to be a superior diagnostic tool, with a patient-based pooled sensitivity of 96% and a pooled specificity of 98%, as well as a lesion-based pooled sensitivity of 97% and pooled specificity of 98% (*5*).

A study on the evaluation of thyroid carcinoma patients for bony metastasis found ^{18}F-NaF PET/CT to be more sensitive than planar bone scanning (*12*). However, a different study showed only a limited osteosclerotic bone reaction from thyroid cancer metastases on ^{18}F-NaF PET (*41*).

Comparison between a standard ^{99m}Tc-based bone scan with and without

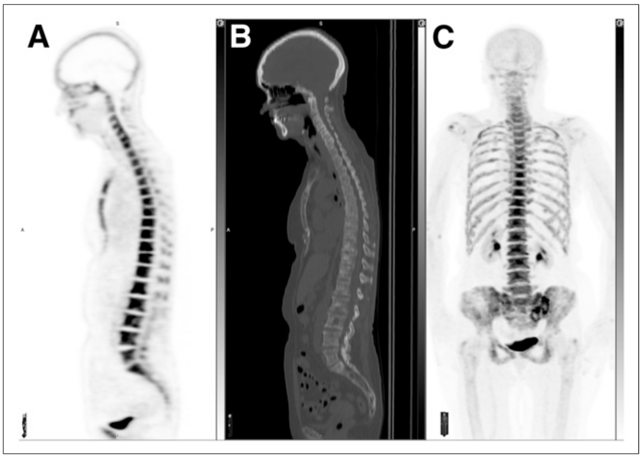

FIGURE 2. An 81-y-old woman with history of metastatic breast cancer. Sagittal ^{18}F-NaF PET (A) and CT (B) images and anterior maximum-intensity projection (C) show diffuse sclerotic metastasis to entire spine and sternum with abnormally increased tracer uptake. Maximum-intensity projection also demonstrates abnormal uptake in ribs and pelvis.

SPECT to ^{18}F-NaF PET to evaluate for vertebral osseous metastasis in lung cancer patients showed a significant difference (*40*). Twelve patients had vertebral metastasis, and the study showed that ^{18}F-NaF resulted in no false-negatives whereas the bone scanning produced 6 false-negatives and SPECT produced one. Further, the results of ^{18}F-NaF PET influenced management in 11% of the study population.

Similarly, in the evaluation of hepatocellular carcinoma by a study from Taiwan, ^{18}F-NaF PET was found to have greater diagnostic and prognostic usefulness than ^{99m}Tc-MDP planar bone scintigraphy. ^{18}F-NaF PET had greater accuracy on a lesion basis (95.7% vs. 75.4%, $P = 0.0001$) (*37*). Additionally, the study found a significant correlation between the presence of ^{18}F-NaF PET/CT–positive bone lesions and overall survival, whereas such a correlation was not observed with bone scans.

Chakraborty et al. found ^{18}F-NaF PET/CT to have a higher sensitivity, specificity, positive predictive value, negative predictive value, and accuracy in detecting bone metastases in urinary bladder carcinoma than conventional ^{99m}Tc-MDP planar bone scans (*36*). Sensitivity, specificity, positive predictive value, negative predictive value, and accuracy were 82.35%, 64.51%, 56%, 86.95%, and 70.83%, respectively, for ^{99m}Tc-MDP planar bone scans; 88.23%, 74.19%, 65.21%, 92%, and 79.16%, respectively, for ^{99m}Tc-MDP SPECT/CT; and 100%, 87.09%, 80.95%, 100%, and 91.66%, respectively, for ^{18}F-NaF PET/CT. Furthermore, ^{18}F-fluoride PET/CT changed management in 17 of 48 patients (35%).

A study on prostate cancer showed that sensitivity, specificity, positive predictive value, and negative predictive value were 70%, 57%, 64%, and 55%, respectively, for planar bone scans; 92%, 82%, 86%, and 90%, respectively, for multiple–field-of-view SPECT; 100%, 62%, 74%, and 100%, respectively, for ^{18}F-fluoride PET; and 100% for all parameters for ^{18}F-fluoride PET/CT (*35*). ^{18}F-fluoride PET/CT was statistically more sensitive and more specific than planar or SPECT bone scans ($P < 0.05$) and more specific than ^{18}F-fluoride PET alone ($P < 0.001$). SPECT was statistically more sensitive and specific than planar bone scans ($P < 0.05$) but was less sensitive than ^{18}F-fluoride PET ($P < 0.05$). Also, ^{18}F-NaF scans detected 81 more lesions, including 34 metastases that were overlooked on planar bone scans.

Another study compared ^{99m}Tc-MDP whole-body bone scans with ^{18}F-NaF PET/CT and ^{18}F-fluoromethylcholine PET/CT (*42*). Poulsen et al. found the sensitivity, specificity, positive and negative predictive values, and accuracy to be as follows: whole-body scanning: 51%, 82%, 86%, 43%, and 61%, respectively; ^{18}F-NaF-PET/CT: 93%, 54%, 82%, 78%, and 81%, respectively; and ^{18}F-fluoromethylcholine PET/CT: 85%, 91%, 95%, 75%, and 87%, respectively. The authors recommended combined ^{18}F-NaF PET/CT and ^{18}F-fluorocholine PET/CT as being accurate in this clinical setting and superior to standard bone scintigraphy. Similar results in other studies have resulted in a call for a change in practice guidelines to prefer ^{18}F-NaF PET/CT and ^{11}C- or ^{18}F-choline PET/CT over ^{99m}Tc-based bone scanning for detection and monitoring of bony metastases of prostate cancer (*43–45*).

Growing research on metastasis detection has shown significantly better sensitivity, specificity, and diagnostic accuracy for ^{18}F-NaF PET or PET/CT than for ^{99m}Tc-MDP bone scintigraphy (*30,33,35,46*). A meta-analysis based on 11 studies encompassing 425 patients to determine the diagnostic accuracy of ^{18}F-NaF PET for detection of metastatic disease showed a sensitivity and specificity of 96.2% and 98.5%, respectively (*5*). Of the 425 patients analyzed on a lesion basis, 225 showed a sensitivity of 96.9% and specificity of 98.0%. Data analysis by receiver-operating-characteristic curves showed the diagnostic accuracy of PET or PET/CT to be significantly higher than that of planar and SPECT bone scintigraphy.

Although the traditionally used ^{99m}Tc-MDP bone scintigraphy has a reasonable sensitivity, the literature shows that the reduced specificity can be improved using SPECT. The accuracy of metastasis detection is further increased with the use of ^{18}F-NaF PET/CT (*47*). Data indicate improved accuracy of bone lesion detection, with a high negative predictive value, for ^{18}F-NaF PET/CT compared with ^{99m}Tc-MDP SPECT and planar ^{99m}Tc-MDP—a finding that has significant clinical implications in ruling out osseous metastatic disease with a high degree of confidence (*9,29,30,40*).

However, a recent study demonstrated that ^{18}F-NaF PET/CT was unable to detect bone metastases within 24 mo of radical prostatectomy in patients with biochemical failure. The report on this study concluded that staging with ^{18}F-NaF PET/CT does not have a superior prognostic value in patients with normal bone scan results in terms of improved patient-related outcomes after radical prostatectomy (*48*).

PET offers a higher resolution, and as a result, ^{18}F-NaF PET is considered more sensitive than the traditionally used ^{99m}Tc-MDP bone scans to detect the minimal osteoblastic activity associated with lytic bone metastases (*27,38,49*). However, since the accumulation of fluoride is not tumor-specific, it has a reduced specificity for detection of metastatic lesions, sometimes making it difficult to differentiate them from benign bone lesions such as degenerative disease, based on the intensity of tracer uptake or SUV. Furthermore, the comparison shows ^{18}F-NaF PET to have a significantly reduced specificity (62%) compared with ^{99m}Tc-MDP SPECT due to the increased sensitivity of PET at detecting bone lesions, which are more likely to be benign and, therefore, result in false-positive findings (*47*). Cancer patients who require a bone scan for metastasis evaluation are often elderly and have coexisting age-related benign bone lesions such as degenerative or arthritic bone disease. These benign bone processes share the same pattern of fluoride uptake as metastases, resulting in more false-positives than seen if evaluated by PET alone. To overcome this problem, low-dose CT is incorporated with hybrid technology, resulting in an improved specificity of 100% with ^{18}F-NaF PET/CT (Fig. 3) (*27*).

In one prospective study with prostate cancer patients, ^{18}F-NaF PET/CT was able to detect a higher number of bone metastases than ^{99m}Tc-MDP bone scintigraphy, with the added advantage of detection at an earlier phase. The number of lesions identified on the first ^{18}F-NaF PET/CT scan and the interval SUV change had a direct correlation with overall survival. As per this study, an increase in SUV by 50% or more correlated with increased mortality (*50*). Another meta-analysis on 14 studies and 507 patients showed ^{18}F-NaF PET/CT to be superior to ^{99m}Tc-MDP bone scintigraphy and SPECT in detecting osseous metastases during staging and restaging of high-risk prostate cancer (*51*).

^{18}F-NaF PETCT is also more accurate than ^{99m}Tc-MDP bone scintigraphy for monitoring bone metastasis from prostate cancer after treatment with ^{223} Ra-chloride (*52*). ^{223}Ra-chloride is a Food and Drug Administration–approved α--emitter used in patients with castration-resistant prostate cancer with bony metastases (*53*). Also, in a study on a small patient population, ^{18}F-NaF PET was superior to ^{99m}Tc-MDP whole-body bone scans for evaluation of treatment response in bone metastasis (*54*).

In conclusion, the literature indicates that ^{18}F-NaF uptake occurs in osteolytic metastasis as well as osteoblastic metastasis (*49,55*).

^{18}F-NaF Versus CT and MRI

Piccardo et al. studied 39 women with breast cancer with bone metastasis and reported that the sensitivity of detection was significantly better for ^{18}F-NaF PET/CT than for CT alone (91% and 77%, respectively) (*27*). However, the specificity of ^{18}F-NaF PET/CT was 91% whereas CT had a specificity of 93%. It has been shown that ^{18}F-NaF PET/CT is superior to contrast-enhanced and non-enhanced chest, abdomen, and pelvis CT and to ^{99m}Tc-MDP bone scans for the detection of occult bone metastasis in patients with prostate cancer (*56*).

In addition, ^{18}F-NaF PET is a useful tool to detect iatrogenic disorders such as bisphosphonate-induced osteonecrosis of the jaw. Current modalities for assessment, such as contrast-enhanced MRI and cone-beam CT, have been proven less accurate for this condition (*57*).

A study by Poulsen et al. used MRI as a gold-standard reference for the detection of bone metastasis in prostate cancer patients. They reported that 114 lesions not detected by MRI were picked up by one or more of the modalities, including whole-body bone scintigraphy, ^{18}F-NaF PET/CT, and ^{18}F-fluoromethylcholine PET/CT. Of these, the most sensitive was ^{18}F-NaF PET/CT, with 68 lesions, whereas 10 lesions were detected by both ^{18}F-NaF PET/CT and ^{18}F-fluoromethylcholine PET/CT (*42*).

A meta-analysis of 14 studies and 507 patients reported ^{18}F-NaF PET/CT to have a diagnostic performance comparable to that of diffusion-weighted MRI (*51*). However, more recent studies have shown significantly better sensitivity, specificity, and overall accuracy than for diffusion-weighted MRI (*58,59*).

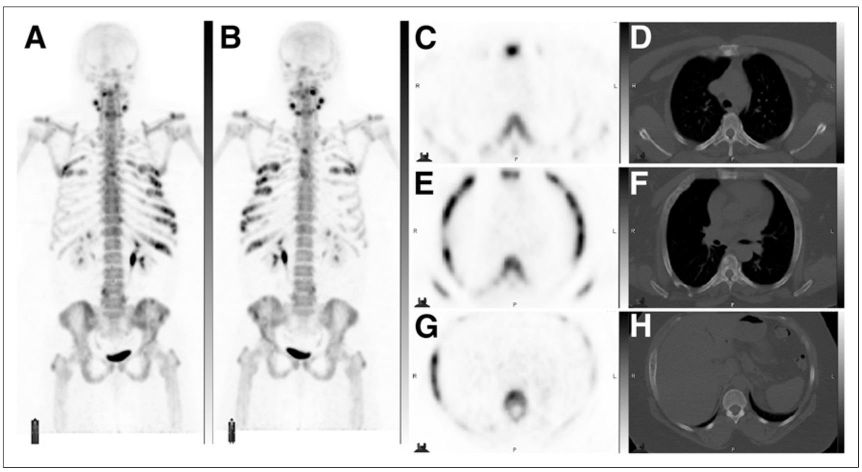

FIGURE 3. A 48-y-old woman with history of plasma cell dyscrasia. (A and B) Anterior and posterior maximum-intensity projections of ^{18}F-NaF PET scan show multifocal areas of abnormally increased tracer uptake in spine, bilateral ribs, and mandible. (C–H) Selected axial PET and CT bone window images show expansile lesions involving bilateral ribs with ground glass density and associated abnormal tracer uptake. These lesions were stable on multiple follow-up scans and were attributable to polyostotic fibrous dysplasia.

^{18}F-NaF Versus ^{18}F-FDG

A published study comparing the detection of bone metastasis by ^{18}F-NaF PET/CT and ^{18}F-FDG PET/CT in head and neck cancer patients at high risk for metastasis found the 2 modalities to have comparable lesion-based sensitivities of 69.4% and 57.1%, respectively, with a P value of 0.126 (*60*). They also had similar areas under the curve of 0.7561 versus 0.7959 ($P = 0.149$). When combined, ^{18}F-NaF PET/CT and ^{18}F-FDG PET/CT demonstrated a significantly better lesion-based sensitivity than that for a single modality ($P < 0.001$). However, a similar advantage was not observed in patient-based analysis, and therefore, their combined use is not advised (*61*).

Krüger et al. studied 126 non–small cell lung cancer patients and reported a comparison of ^{18}F-NaF PET with ^{18}F-FDG PET/CT for detection of bone metastasis (*10*). They found concordant metastases diagnosed in 13 of 18 patients. Interestingly, ^{18}F-FDG PET/CT detected a higher absolute number of bone metastases than ^{18}F-NaF PET (73 vs. 55, $P < 0.05$). However, ^{18}F-NaF PET diagnosed more patients with bone metastases, in that 4 patients showed positive findings on ^{18}F-NaF PET but negative findings on ^{18}F-FDG PET/CT.

Iagaru et al. compared ^{18}F-NaF and ^{18}F-FDG PET/CT for detection of skeletal metastasis in 52 patients (*11*). They reported ^{18}F-NaF PET/CT to have superior detection of skeletal metastatic disease (24 vs. 16) as well as better image quality. However, the study also showed that extraskeletal metastasis detection by ^{18}F-FDG PET/CT could alter management. Therefore, a combined approach to disease evaluation was suggested. Iagaru et al. conducted another study to test a combination of ^{18}F-NaF PET/CT and ^{18}F-FDG PET/CT as an imaging modality for cancer patients (*61*). They reported that the combined approach missed none of the lesions detected by ^{18}F-FDG PET/CT and only one skull lesion detected by ^{18}F-NaF PET/CT alone.

A recent retrospective study comparing ^{18}F-NaF PET/CT and ^{18}F-FDG PET/CT in detection of skull-base invasion and bony metastases in nasopharyngeal cancer detected more osseous metastases and had a more accurate assessment of skull-base invasion on ^{18}F-NaF PET/CT than on ^{18}F-FDG PET/CT. For detecting skull-base invasion, ^{18}F-NaF PET/CT had a sensitivity, specificity, accuracy, positive predictive value, and negative predictive value of 100%, 94.7%, 97.8%, 96.3%, and 100%, respectively, whereas for ^{18}F-FDG PET/CT these measures were 65.4%, 100%, 80%, 100%, and 67.9%, respectively. The sensitivity and specificity for detecting bone metastatic lesions were 98.3%, and 65.7%, respectively, for ^{18}F-NaF PET/CT and 42.9%, and 97.1%, respectively, for ^{18}F-FDG PET/CT (Table 2) (*62*).

Studies comparing ^{18}F-NaF PET/CT and ^{18}F-FDG PET/CT in multiple-myeloma patients found only a 39% correlation for disease assessment, with 343 and 135 lesions picked up by ^{18}F-NaF PET/CT and ^{18}F-FDG PET/CT,

TABLE 2
Studies Comparing ^{18}F-NaF with Other Radiotracers

Study	Parameter	Sn	Sp	PPV	NPV	Ac
Meta-analysis of ^{18}F-NaF in both benign and malignant lesions (*5*)	Patient-based pooled	96%	98%			
	Lesion-based pooled	97%	98%			
Bone metastasis detection in hepatocellular carcinoma (*37*)	^{99m}Tc-MDP	73.3%	79.2%	86.8%	61.3%	75.4%
	^{18}F-NaF PET/CT	93.3%	100%	100%	88.9%	97.5%
Bone metastasis detection in urinary bladder cancer (*36*)	^{99m}Tc-MDP	82.35%	64.51%	56%	86.95%	70.83%
	^{99m}Tc-MDP SPECT/CT	88.23%	74.19%	65.21%	92%	79.16%
	^{18}F-NaF PET/CT	100%	87.09%	80.95%	100%	91.66%
High-risk prostate cancer (*35*)	^{99m}Tc-MDP	70%	57%	64%	55%	
	^{99m}Tc-MDP SPECT/CT	92%	82%	86%	90%	
	^{18}F-NaF PET	100%	62%	74%	100%	
	^{18}F-NaF PET/CT	100%	100%	100%	100%	
Spine metastasis in prostate cancer (*42*)	^{99m}Tc-MDP	51%	82%	86%	43%	61%
	^{18}F-NaF PET/CT	93%	54%	82%	78%	81%
	^{18}F-fluoromethylcholine PET/CT	85%	91%	95%	75%	87%
Bone metastasis detection in head and neck cancer (*60*)	^{18}F-NaF PET/CT	69.4%				
	^{18}F-FDG PET/CT	57.1%				
Detection of skull-base invasion in nasopharyngeal cancer (*62*)	^{18}F-NaF PET/CT	100%	94.7%	96.3%	100%	97.8%
	^{18}F-FDG PET/CT	65.4%	100%	100%	67.9%	80%
Detection of bone metastasis in nasopharyngeal cancer (*62*)	^{18}F-NaF PET/CT	98.3%	65.7%			
	^{18}F-FDG PET/CT	42.9%	97.1%			

Sn = sensitivity; Sp = specificity; PPV = positive predictive value; NPV = negative predictive value; Ac = accuracy.

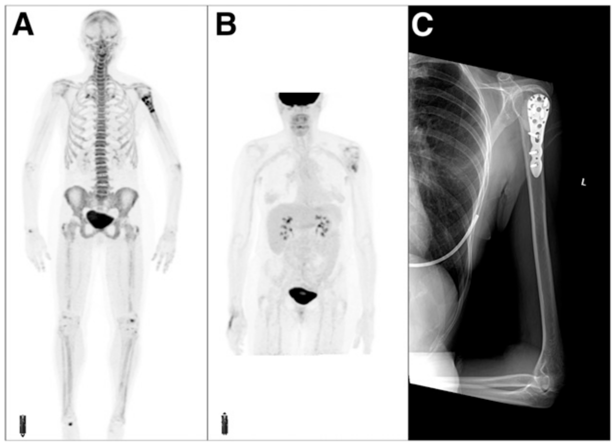

FIGURE 4. A 58-y-old woman with history of metastatic colorectal cancer, seen after radiation therapy and placement of fixation hardware for lytic metastasis to left proximal humerus. Anterior maximum-intensity projection of ^{18}F-NaF (A) and ^{18}F-FDG (B) PET scans shows heterogeneously increased tracer uptake in left proximal humerus secondary to bone remodeling. No other area of abnormal tracer activity is seen elsewhere. (C) X-ray of left humerus shows cement and fixation hardware.

respectively (*63*). Interestingly, 3 patients who showed multiple focal lesions on ^{18}F-FDG PET/CT had no identifiable lesions on ^{18}F-NaF PET/CT. In addition, evaluation of the pelvic area with ^{18}F-NaF and ^{18}F-FDG PET/CT demonstrated 24 and 77 lesions, respectively.

In one prospective study on patients with prostate and breast cancers, ^{18}F-NaF/^{18}F-FDG PET/CT was superior to whole-body MRI and ^{99m}Tc-MDP scintigraphy for detection of bone metastasis. The performance of ^{18}F-NaF/^{18}F-FDG PET/CT was similar to a combination of whole-body MRI and bone scintigraphy (Fig. 4) (*64*).

CONCLUSION

Detection of bony metastases in patients with malignancy is a matter of high clinical importance as it can significantly impact treatment and outcome. ^{18}F-NaF PET has shown excellent diagnostic performance in the detection of bone metastases. Through advancements in PET scanners in recent decades, ^{18}F-NaF PET is now feasible and its radiation dose is comparable to a conventional ^{99m}Tc-MDP bone scan. By having a better spatial resolution, better image quality, higher target-to-background contrast, and higher sensitivity, ^{18}F-NaF PET is superior to a conventional ^{99m}Tc-MDP bone scan. It has also shown superiority to other imaging modalities, including CT, MRI, and ^{18}F-FDG PET/CT. The challenge posed by the low specificity of this modality has been partially solved by using simultaneous anatomic imaging as a part of PET/CT or PET/MRI. Further, the development of new scanners and reconstruction methods will make it possible to perform ^{18}F-NaF PET with a much lower dose. Currently, ^{18}F-NaF PET/CT scans are not being reimbursed by the Centers for Medicare and Medicaid Services, and additional prospective studies are needed to demonstrate the clinical impact of ^{18}F-NaF PET/CT in various malignancies.

DISCLOSURE

No potential conflict of interest relevant to this article was reported.

REFERENCES

1. Mick CG, James T, Hill JD, Williams P, Perry M. Molecular imaging in oncology: ^{18}F-sodium fluoride PET imaging of osseous metastatic disease. *AJR.* 2014;203:263–271.
2. Harley SJ, Hoffmann R, Bartholomeusz D, et al. 18-fluoride labeled sodium fluoride positron emission tomography with computer tomography: the impact of pretreatment staging in intermediate- and high-risk prostate cancer. *Prostate Int.* 2018;6:50–54.
3. Panagiotidis E, Lam K, Mistry A, Seshadri N, Vinjamuri S. Skeletal metastases and benign mimics on NaF PET/CT: a pictorial review. *AJR.* 2018;211:W64–W74.
4. Shen CT, Qiu ZL, Han TT, Luo QY. Performance of ^{18}F-fluoride PET or PET/CT for the detection of bone metastases: a meta-analysis. *Clin Nucl Med.* 2015;40:103–110.
5. Tateishi U, Morita S, Taguri M, et al. A meta-analysis of ^{18}F-fluoride positron emission tomography for assessment of metastatic bone tumor. *Ann Nucl Med.* 2010;24:523–531.
6. Hillner BE, Siegel BA, Hanna L, Duan F, Quinn B, Shields AF. ^{18}F-fluoride PET used for treatment monitoring of systemic cancer therapy: results from the National Oncologic PET Registry. *J Nucl Med.* 2015;56:222–228.
7. Hillner BE, Siegel BA, Hanna L, et al. Impact of ^{18}F-fluoride PET on intended management of patients with cancers other than prostate cancer: results from the National Oncologic PET Registry. *J Nucl Med.* 2014;55:1054–1061.
8. Hillner BE, Siegel BA, Hanna L, Duan F, Shields AF, Coleman RE. Impact of ^{18}F-fluoride PET in patients with known prostate cancer: initial results from the National Oncologic PET Registry. *J Nucl Med.* 2014;55:574–581.
9. Bortot DC, Amorim BJ, Oki GC, et al. ^{18}F-fluoride PET/CT is highly effective for excluding bone metastases even in patients with equivocal bone scintigraphy. *Eur J Nucl Med Mol Imaging.* 2012;39:1730–1736.
10. Krüger S, Buck AK, Mottaghy FM, et al. Detection of bone metastases in patients with lung cancer: ^{99m}Tc-MDP planar bone scintigraphy, ^{18}F-fluoride PET or ^{18}F-FDG PET/CT. *Eur J Nucl Med Mol Imaging.* 2009;36:1807–1812.
11. Iagaru A, Mittra E, Dick DW, Gambhir SS. Prospective evaluation of ^{99m}Tc MDP scintigraphy, ^{18}F NaF PET/CT, and ^{18}F FDG PET/CT for detection of skeletal metastases. *Mol Imaging Biol.* 2012;14:252–259.
12. Ota N, Kato K, Iwano S, et al. Comparison of ^{18}F-fluoride PET/CT, ^{18}F-FDG PET/CT and bone scintigraphy (planar and SPECT) in detection of bone metastases of differentiated thyroid cancer: a pilot study. *Br J Radiol.* 2014;87:20130444.
13. Czernin J, Satyamurthy N, Schiepers C. Molecular mechanisms of bone ^{18}F-NaF deposition. *J Nucl Med.* 2010;51:1826–1829.
14. Decision memo for positron emission tomography (NaF-18) to identify bone metastasis of cancer (CAG-00065R). Centers for Medicare and Medicaid Services website. https://www.cms.gov/medicare-coverage-database/details/nca-decision-memo.aspx?NCAId=233. Assessed January 22, 2020.
15. Hillner BE, Hanna L, Makineni R, et al. Intended versus inferred treatment after ^{18}F-fluoride PET performed for evaluation of osseous metastatic disease in the National Oncologic PET Registry. *J Nucl Med.* 2018;59:421–426.
16. Segall G, Delbeke D, Stabin MG, et al. SNM practice guideline for sodium ^{18}F-fluoride PET/CT bone scans 1.0. *J Nucl Med.* 2010;51:1813–1820.
17. Jadvar H, Colletti PM, Delgado-Bolton R, et al. Appropriate use criteria for ^{18}F-FDG PET/CT in restaging and treatment response assessment of malignant disease. *J Nucl Med.* 2017;58:2026–2037.
18. Langsteger W, Rezaee A, Pirich C, Beheshti M. ^{18}F-NaF-PET/CT and ^{99m}Tc-MDP bone scintigraphy in the detection of bone metastases in prostate cancer. *Semin Nucl Med.* 2016;46:491–501.
19. Beheshti M, Mottaghy FM, Paycha F, et al. ^{18}F-NaF PET/CT: EANM procedure guidelines for bone imaging. *Eur J Nucl Med Mol Imaging.* 2015;42:1767–1777.
20. Bastawrous S, Bhargava P, Behnia F, Djang DS, Haseley DR. Newer PET application with an old tracer: role of ^{18}F-NaF skeletal PET/CT in oncologic practice. *Radiographics.* 2014;34:1295–1316.

21. Grant FD, Fahey FH, Packard AB, Davis RT, Alavi A, Treves ST. Skeletal PET with ^{18}F-fluoride: applying new technology to an old tracer. *J Nucl Med.* 2008;49:68–78.
22. Vali R, Beheshti M, Waldenberger P, et al. Assessment of malignant and benign bone lesions by static F-18 fluoride PET-CT: additional value of SUV! [abstract]. *J Nucl Med.* 2008;49(suppl):150P.
23. Muzahir S, Jeraj R, Liu G, et al. Differentiation of metastatic vs degenerative joint disease using semi-quantitative analysis with ^{18}F-NaF PET/CT in castrate resistant prostate cancer patients. *Am J Nucl Med Mol Imaging.* 2015;5:162–168.
24. Oldan JD, Hawkins AS, Chin BB. ^{18}F sodium fluoride PET/CT in patients with prostate cancer: quantification of normal tissues, benign degenerative lesions, and malignant lesions. *World J Nucl Med.* 2016;15:102–108.
25. Beheshti M, Mottaghy FM, Paycha F, et al. Correction to: ^{18}F-NaF PET/CT: EANM procedure guidelines for bone imaging. *Eur J Nucl Med Mol Imaging.* 2018;45:322.
26. Park-Holohan SJ, Blake GM, Fogelman I. Quantitative studies of bone using ^{18}F-fluoride and ^{99m}Tc-methylene diphosphonate: evaluation of renal and whole-blood kinetics. *Nucl Med Commun.* 2001;22:1037–1044.
27. Piccardo A, Altrinetti V, Bacigalupo L, et al. Detection of metastatic bone lesions in breast cancer patients: fused ^{18}F-Fluoride-PET/MDCT has higher accuracy than MDCT—preliminary experience. *Eur J Radiol.* 2012;81:2632–2638.
28. Iagaru A, Mittra E, Mosci C, et al. Combined ^{18}F-fluoride and ^{18}F-FDG PET/CT scanning for evaluation of malignancy: results of an international multicenter trial. *J Nucl Med.* 2013;54:176–183.
29. Damle NA, Bal C, Bandopadhyaya GP, et al. The role of ^{18}F-fluoride PET-CT in the detection of bone metastases in patients with breast, lung and prostate carcinoma: a comparison with FDG PET/CT and ^{99m}Tc-MDP bone scan. *Jpn J Radiol.* 2013;31:262–269.
30. Withofs N, Grayet B, Tancredi T, et al. ^{18}F-fluoride PET/CT for assessing bone involvement in prostate and breast cancers. *Nucl Med Commun.* 2011;32:168–176.
31. Segall GM. PET/CT with sodium ^{18}F-fluoride for management of patients with prostate cancer. *J Nucl Med.* 2014;55:531–533.
32. Cook GJ, Fogelman I. Detection of bone metastases in cancer patients by ^{18}F-fluoride and ^{18}F-fluorodeoxyglucose positron emission tomography. *Q J Nucl Med.* 2001;45:47–52.
33. Schirrmeister H, Guhlmann A, Elsner K, et al. Sensitivity in detecting osseous lesions depends on anatomic localization: planar bone scintigraphy versus ^{18}F PET. *J Nucl Med.* 1999;40:1623–1629.
34. Hetzel M, Arslandemir C, Konig HH, et al. F-18 NaF PET for detection of bone metastases in lung cancer: accuracy, cost-effectiveness, and impact on patient management. *J Bone Miner Res.* 2003;18:2206–2214.
35. Even-Sapir E, Metser U, Mishani E, Lievshitz G, Lerman H, Leibovitch I. The detection of bone metastases in patients with high-risk prostate cancer: ^{99m}Tc-MDP planar bone scintigraphy, single- and multi-field-of-view SPECT, ^{18}F-fluoride PET, and ^{18}F-fluoride PET/CT. *J Nucl Med.* 2006;47:287–297.
36. Chakraborty D, Bhattacharya A, Mete UK, Mittal BR. Comparison of ^{18}F fluoride PET/CT and ^{99m}Tc-MDP bone scan in the detection of skeletal metastases in urinary bladder carcinoma. *Clin Nucl Med.* 2013;38:616–621.
37. Yen RF, Chen CY, Cheng MF, et al. The diagnostic and prognostic effectiveness of F-18 sodium fluoride PET-CT in detecting bone metastases for hepatocellular carcinoma patients. *Nucl Med Commun.* 2010;31:637–645.
38. Schirrmeister H, Guhlmann A, Kotzerke J, et al. Early detection and accurate description of extent of metastatic bone disease in breast cancer with fluoride ion and positron emission tomography. *J Clin Oncol.* 1999;17:2381–2389.
39. Iagaru A, Young P, Mittra E, Dick DW, Herfkens R, Gambhir SS. Pilot prospective evaluation of ^{99m}Tc-MDP scintigraphy, ^{18}F NaF PET/CT, ^{18}F FDG PET/CT and whole-body MRI for detection of skeletal metastases. *Clin Nucl Med.* 2013;38:e290–e296.
40. Schirrmeister H, Glatting G, Hetzel J, et al. Prospective evaluation of the clinical value of planar bone scans, SPECT, and ^{18}F-labeled NaF PET in newly diagnosed lung cancer. *J Nucl Med.* 2001;42:1800–1804.
41. Schirrmeister H, Buck A, Guhlmann A, Reske SN. Anatomical distribution and sclerotic activity of bone metastases from thyroid cancer assessed with F-18 sodium fluoride positron emission tomography. *Thyroid.* 2001;11:677–683.
42. Poulsen MH, Petersen H, Hoilund-Carlsen PF, et al. Spine metastases in prostate cancer: comparison of technetium-99m-MDP whole-body bone scintigraphy, [^{18}F]choline positron emission tomography(PET)/computed tomography (CT) and [^{18}F]NaF PET/CT. *BJU Int.* 2014;114:818–823.
43. Wondergem M, van der Zant FM, van der Ploeg T, Knol RJ. A literature review of ^{18}F-fluoride PET/CT and ^{18}F-choline or ^{11}C-choline PET/CT for detection of bone metastases in patients with prostate cancer. *Nucl Med Commun.* 2013;34:935–945.
44. Kjölhede H, Ahlgren G, Almquist H, et al. Combined ^{18}F-fluorocholine and ^{18}F-fluoride positron emission tomography/computed tomography imaging for staging of high-risk prostate cancer. *BJU Int.* 2012;110:1501–1506.
45. Langsteger W, Balogova S, Huchet V, et al. Fluorocholine (^{18}F) and sodium fluoride (^{18}F) PET/CT in the detection of prostate cancer: prospective comparison of diagnostic performance determined by masked reading. *Q J Nucl Med Mol Imaging.* 2011;55:448–457.
46. Kawaguchi M, Tateishi U, Shizukuishi K, Suzuki A, Inoue T. ^{18}F-fluoride uptake in bone metastasis: morphologic and metabolic analysis on integrated PET/CT. *Ann Nucl Med.* 2010;24:241–247.
47. Kulshrestha RK, Vinjamuri S, England A, Nightingale J, Hogg P. The role of ^{18}F-sodium fluoride PET/CT bone scans in the diagnosis of metastatic bone disease from breast and prostate cancer. *J Nucl Med Technol.* 2016;44:217–222.
48. Zacho H, Jochumsen MR, Langkilde NC, et al. No added value of ^{18}F-sodium fluoride PET/CT for the detection of bone metastases in patients with newly diagnosed prostate cancer with normal bone scintigraphy. *J Nucl Med.* 2019;60:1713–1716.
49. Petrén-Mallmin M, Andreasson I, Ljunggren O, et al. Skeletal metastases from breast cancer: uptake of ^{18}F-fluoride measured with positron emission tomography in correlation with CT. *Skeletal Radiol.* 1998;27:72–76.
50. Apolo AB, Lindenberg L, Shih JH, et al. Prospective study evaluating Na^{18}F PET/CT in predicting clinical outcomes and survival in advanced prostate cancer. *J Nucl Med.* 2016;57:886–892.
51. Sheikhbahaei S, Jones KM, Werner RA, et al. ^{18}F-NaF-PET/CT for the detection of bone metastasis in prostate cancer: a meta-analysis of diagnostic accuracy studies. *Ann Nucl Med.* 2019;33:351–361.
52. Cook G Jr, Parker C, Chua S, Johnson B, Aksnes AK, Lewington VJ. ^{18}F-fluoride PET: changes in uptake as a method to assess response in bone metastases from castrate-resistant prostate cancer patients treated with ^{223}Ra-chloride (Alpharadin). *EJNMMI Res.* 2011;1:4.
53. Gupta N, Devgan A, Bansal I, et al. Usefulness of radium-223 in patients with bone metastases. *Proc Bayl Univ Med Cent.* 2017;30:424–426.
54. Zukotynski KA, Kim CK, Gerbaudo VH, et al. ^{18}F-FDG-PET/CT and ^{18}F-NaF-PET/CT in men with castrate-resistant prostate cancer. *Am J Nucl Med Mol Imaging.* 2014;5:72–82.
55. Araz M, Aras G, Kucuk ON. The role of ^{18}F-NaF PET/CT in metastatic bone disease. *J Bone Oncol.* 2015;4:92–97.
56. Jadvar H, Desai B, Ji L, et al. Prospective evaluation of ^{18}F-NaF and ^{18}F-FDG PET/CT in detection of occult metastatic disease in biochemical recurrence of prostate cancer. *Clin Nucl Med.* 2012;37:637–643.
57. Kurata S, Tateishi U, Shizukuishi K, et al. Assessment of atherosclerosis in oncologic patients using ^{18}F-fluoride PET/CT. *Ann Nucl Med.* 2013;27:481–486.
58. Zacho HD, Nielsen JB, Afshar-Oromieh A, et al. Prospective comparison of ^{68}Ga-PSMA PET/CT, ^{18}F-sodium fluoride PET/CT and diffusion weighted-MRI at for the detection of bone metastases in biochemically recurrent prostate cancer. *Eur J Nucl Med Mol Imaging.* 2018;45:1884–1897.
59. Dyrberg E, Hendel HW, Huynh THV, et al. ^{68}Ga-PSMA-PET/CT in comparison with ^{18}F-fluoride-PET/CT and whole-body MRI for the detection of bone metastases in patients with prostate cancer: a prospective diagnostic accuracy study. *Eur Radiol.* 2019;29:1221–1230.
60. Chan SC, Wang HM, Ng SH, et al. Utility of ^{18}F-fluoride PET/CT and ^{18}F-FDG PET/CT in the detection of bony metastases in heightened-risk head and neck cancer patients. *J Nucl Med.* 2012;53:1730–1735.
61. Iagaru A, Mittra E, Yaghoubi SS, et al. Novel strategy for a cocktail ^{18}F-fluoride and ^{18}F-FDG PET/CT scan for evaluation of malignancy: results of the pilot-phase study. *J Nucl Med.* 2009;50:501–505.
62. Zhang Y, Chen Y, Huang Z, Zhang L, Wan Q, Lei L. Comparison of ^{18}F-NaF PET/CT and ^{18}F-FDG PET/CT for detection of skull-base invasion and osseous metastases in nasopharyngeal carcinoma. *Contrast Media Mol Imaging.* 2018;2018:8271313.
63. Sachpekidis C, Goldschmidt H, Hose D, et al. PET/CT studies of multiple myeloma using ^{18}F-FDG and ^{18}F-NaF: comparison of distribution patterns and tracers' pharmacokinetics. *Eur J Nucl Med Mol Imaging.* 2014;41:1343–1353.
64. Minamimoto R, Loening A, Jamali M, et al. Prospective comparison of ^{99m}Tc-MDP scintigraphy, combined ^{18}F-NaF and ^{18}F-FDG PET/CT, and whole-body MRI in patients with breast and prostate cancer. *J Nucl Med.* 2015;56:1862–1868.